

Nanoscale

Accepted Manuscript



This is an *Accepted Manuscript*, which has been through the Royal Society of Chemistry peer review process and has been accepted for publication.

Accepted Manuscripts are published online shortly after acceptance, before technical editing, formatting and proof reading. Using this free service, authors can make their results available to the community, in citable form, before we publish the edited article. We will replace this *Accepted Manuscript* with the edited and formatted *Advance Article* as soon as it is available.

You can find more information about *Accepted Manuscripts* in the [Information for Authors](#).

Please note that technical editing may introduce minor changes to the text and/or graphics, which may alter content. The journal's standard [Terms & Conditions](#) and the [Ethical guidelines](#) still apply. In no event shall the Royal Society of Chemistry be held responsible for any errors or omissions in this *Accepted Manuscript* or any consequences arising from the use of any information it contains.

Two-Color SERS Microscopy for Protein Co-localization in Prostate Tissue with Primary Antibody-Protein A/G-Gold Nanocluster Conjugates

Mohammad Salehi¹, Lilli Schneider¹, Philipp Ströbel², Alexander Marx³, Jens Packeisen⁴, Sebastian Schlücker^{1,5}*

¹ Department of Physics, University of Osnabrück, Barbarastr. 7, 49069 Osnabrück, Germany;

² Institute of Pathology, Faculty of Medicine, University of Göttingen, Robert-Koch-Str. 40, 37075 Göttingen, Germany

³ Institute of Pathology, Medical Faculty Mannheim, University of Heidelberg, Theodor-Kutzer-Ufer 1-3, 68167 Mannheim, Germany

⁴ Medical Center, Rheiner Landstraße 91, 49078 Osnabrück, Germany

⁵ Physical Chemistry, Faculty of Chemistry and Center for Nanointegration (CENIDE), University of Duisburg-Essen, Universitätsstr. 5, 45141 Essen, Germany; email: sebastian.schluecker@uni-due.de

KEYWORDS: immunohistochemistry, staining, gold nanoparticle clusters, prostate cancer, tissue imaging, Raman, SERS

SERS microscopy is a novel staining technique in immunohistochemistry, which is based on antibodies labeled with functionalized noble metal colloids called SERS labels or nanotags for optical detection. Conventional covalent bioconjugation of these SERS labels cannot prevent blocking of the antigen recognition sites of the antibody. We present a rational chemical design for SERS label/antibody conjugates which addresses this issue. Highly sensitive, silica-coated gold nanoparticle clusters as SERS labels are non-covalently conjugated to primary antibodies by using the chimeric protein A/G, which selectively recognizes the Fc part of antibodies and therefore prevents blocking of the antigen recognition sites. In proof-of-concept two-color imaging experiments for the co-localization of p63 and PSA on non-neoplastic prostate tissue FFPE specimens, we demonstrate the specificity and signal brightness of these rationally designed primary antibody-protein A/G-gold nanocluster conjugates.

Introduction

SERS microscopy (SERS, surface-enhanced Raman scattering) is a novel optical imaging method for tissue diagnostics.^[1-6] The concept for protein localization is the same as in immunohistochemistry (IHC) and immunofluorescence, i.e., the target antigen is recognized by a labeled antibody. In immuno-SERS microscopy, the corresponding antibodies are labeled by chemically functionalized noble metal colloids (SERS labels or nanotags), i.e., gold or silver metal nanoparticles with organic Raman reporter molecules chemisorbed on their surface, for optical localization.^[6-7] The reporter molecules provide the characteristic “molecular fingerprint” for the identification of the label, while the colloid provides the necessary signal enhancement upon excitation of a localized surface plasmon resonance (LSPR). A central advantage of Raman/SERS-based detection schemes is their enormous spectral multiplexing capacity for multi-color IHC.

How does SERS enable multi-color IHC?

Fluorescence and Raman spectra arise from fundamentally different physical processes: fluorescence involves electronic transitions while vibrational Raman scattering involves transitions between vibrational energy levels. Figure 1 shows the spectral emission profile from a fluorophore (Cy5) in comparison with the Raman spectrum from a SERS label. The

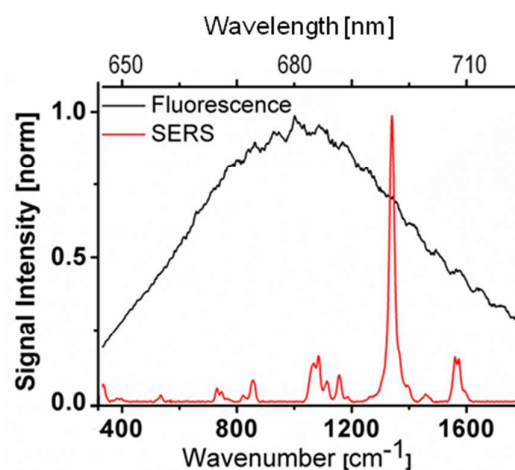


Figure 1: Comparison of spectral emission profiles: fluorescence from Cy5 and SERS from 4-NTB on AuNPs excited with 632.8 nm laser radiation. The SERS spectrum exhibits several narrow vibrational Raman bands, which is the basis of spectral multiplexing for multi-color IHC.

FWHM (full width at half maximum) of the broad fluorescence emission (black solid line), centered around 675-680 nm, is about 40 nm. The multiplexing capacity of fluorescent dyes is limited due to these broad emission profiles and the resulting spectral overlap between them. In contrast, the Raman signature from a SERS label (red solid line), comprising Raman reporter molecules chemisorbed on the surface of a metal colloid, exhibits multiple narrow peaks with a FWHM of typically 5-20 cm^{-1} (bottom scale in Fig. 1) or about 0.5-2 nm (top scale in Fig. 1). The line width of

vibrational Raman bands is therefore about 20-80 times smaller compared with the broad emission profiles of molecular fluorophores; this is the physical basis for spectral multiplexing with SERS labels.

Different colors for spectral multiplexing in fluorescence applications including microscopy are obtained by a set of fluorescent dye molecules with distinct spectral emission profiles. Usually the excitation wavelength for a particular dye is matched to the maximum of its electronic absorption. In contrast, it is not necessary to use different excitation wavelengths in SERS: the Raman spectra of all SERS labels can be excited generated with only a single laser excitation wavelength. Spectrally distinct SERS signatures are obtained by simply changing the Raman reporter molecules on the surface of the metal colloid since each reporter molecule exhibits a unique vibrational fingerprint for spectral identification. The metal nanoparticle enhances the Raman scattering of the reporter molecules by acting as an “optical amplifier” (nanoantenna) upon excitation of the particle’s localized surface plasmon resonance.

Figure 2 shows the SERS spectra of two different SERS labels comprising aromatic thiols present as a self-assembled monolayer (SAM) on the surface of gold nanoparticles (AuNPs). The two Raman reporter molecules are 4-nitrothiobenzoic acid (4-NTB, red solid line) and 4-mercaptobenzoic acid (4-MBA, green solid line), respectively. Each vibrational Raman peak in the SERS spectrum can be assigned to a particular vibration or normal mode of the corresponding molecule. For instance, the Raman peak at about

1340 cm^{-1} in the SERS spectrum of 4-NTB can be assigned to the symmetric nitro stretching vibration, while the Raman peak at about 1590 cm^{-1} in the SERS spectrum of 4-MBA is due to a phenyl ring mode. Since unique and spectrally separated Raman marker bands for both SERS labels are available (Fig. 2), a univariate

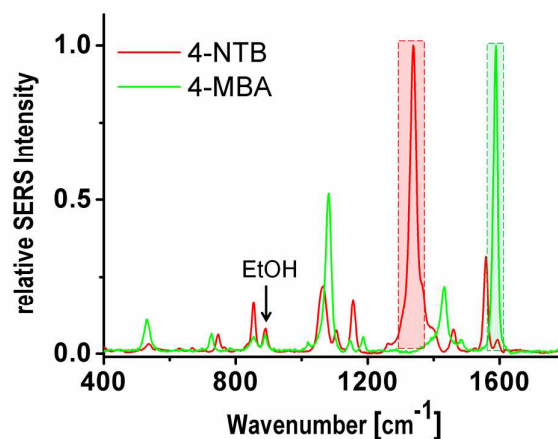


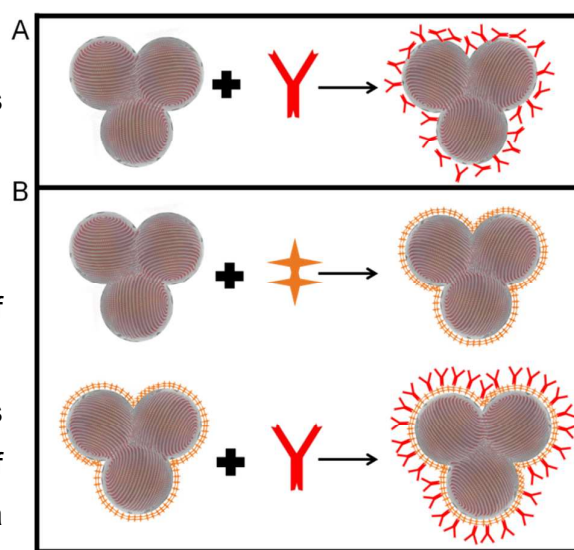
Figure 2: SERS signatures of two different SERS labels comprising two different aromatic thiols present as a SAM on the surface of AuNPs: 4-nitrothiobenzoic acid (4-NTB) and 4-mercaptobenzoic acid (4-MBA). The colloidal SERS particles were dispersed in ethanol.

approach based on the integrated Raman intensities of single peaks – here around 1340 cm^{-1} (4-NTB, red) and around 1590 cm^{-1} (4-MBA, green) – is sufficient for spectral discrimination in a two-color SERS microscopic experiment employing 4-NTB- and 4-MBA-based SERS labels.

Which SERS labels are very bright and exhibit even single-particle sensitivity?

The brightness of SERS labels depends on the scattering properties of both the metal colloid and the Raman reporter molecules on the metal surface. For instance, single solid AuNPs have scattering cross sections which are too low for efficient SERS detection with short ($\ll 1\text{ sec}$) acquisition times.^[8] In contrast, clusters of solid AuNPs such as dimers and trimers exhibit a significantly larger SERS signal strength than individual solid AuNPs due to the presence of “hot spots” in the particle junctions.^[9-11] Raman reporter molecules present in such “hot spots”, i.e., highly localized regions with extremely high electric field enhancements, contribute dominantly to the overall SERS signal of the entire cluster.

Scheme 1 left shows silica-coated trimers of solid AuNP covered with a SAM of Raman reporter molecules. The silica (“glass”) coating is a protective shell, which additionally holds the solid AuNPs together; a close spacing between the AuNPs is important for efficient generation of SERS via “hot spots” since the electric field enhancement decreases rapidly with an increasing gap between the NPs. We have recently demonstrated that silica-coated trimers of 60 nm AuNPs exhibit single-particle sensitivity within 30 msec laser illumination and a quasi-isotropic optical response, i.e., a SERS



Scheme 1: Glass-encapsulated clusters of solid AuNPs coated with a SAM of Raman reporter molecules (left) are bright SERS labels with single-particle SERS sensitivity. (A) Uncontrolled binding of the antibody onto the glass surface of the SERS NP clusters. Due to the uncontrolled orientation of the antibodies, antigen binding sites may be blocked. (B) Controlled binding and directed orientation of the antibodies onto the silica surface of the SERS NP cluster via coating with protein A/G (top), which exhibits multiple binding sites for the Fc fragment of the antibody (bottom). In this case, all antigen binding sites are accessible.

signal which is quasi-independent of the polarization direction of the incident laser beam.^[12] Single-particle sensitivity is relevant from a diagnostic point of view since otherwise unwanted false-negative results can be generated if the antibody-NP conjugate binds to the target but does not yield a detectable signal within the acquisition time.^[8]

How to ensure efficient target recognition by antibody-SERS label conjugates?

Molecular recognition of the target antigen by the antigen-recognition sites of the antibody is highly important for obtaining molecular specificity and therefore reliable diagnostic results in IHC. Blocking of these sites diminishes the capability of the primary antibody-SERS label conjugate to recognize the corresponding target; this may lead to unwanted false-negative results since the extent of specific binding is reduced. Previous designs of antibody-SERS label conjugates (Scheme 1A) have not addressed this issue since they usually involve covalent conjugation of the antibody to the surface of the SERS label. For instance, primary amino groups (NH₂) from lysine residues of the antibody can be conjugated to activated carboxylic groups.^[13-15] However, conventional bioconjugation schemes^[16] do not provide site-specificity, i.e., there is no control over targeting a particular amino acid residue: the targeted lysine residues might be close to the Fc part of the receptor (preferred) or within the antigen recognition sites (non-preferred). Overall, this uncontrolled binding in terms of missing site-specificity may result in a “scrambled” orientation of the antibodies on the silica surface of the SERS NP cluster (Scheme 1A). In contrast, the design presented here (Scheme 1B) avoids this problem by using the chimeric protein A/G, which exhibits multiple bindings to the Fc domain of the antibody.^[17,18] Coating the silica surface of the SERS labels with protein A/G therefore does not block the antigen recognition sites of the antibody.

In the present proof-of-concept study we employ such primary antibody-protein A/G-gold nanocluster conjugates (Scheme 1B) for SERS microscopy. Non-neoplastic prostatic tissue was chosen for establishing this methodology. Localization of the basal cell marker p63 is a clear test whether immuno-SERS microscopy provides the necessary specificity for selectively staining the nuclei of the basal cells. Prostate-specific antigen (PSA) was chosen as a second target since it is highly expressed in the entire epithelium; it already has served as a test system in previous immuno-SERS studies.^[19,20] In addition to one-color SERS microscopy, we also employ two

spectrally distinct SERS labels (Fig. 2) in two-color SERS microscopic experiments for the co-localization of p63 and PSA in the non-neoplastic prostate.

Results and discussion:

SERS labels and primary antibody-protein A/G-gold nanocluster conjugates

Highly purified silica-encapsulated clusters of 60 nm AuNPs were prepared as described in the materials and methods section. The transmission electron microscopy (TEM) image in Figure 3 shows the high purity of the colloid, which contains only small, highly SERS-active clusters such as dimers and trimers. In contrast, monomers, which are only weakly SERS-active, are not present. The introduction of functional groups and spacers on the surface of the silica shell of the SERS labels and the subsequent bioconjugation to antibodies is described in the materials and methods section.

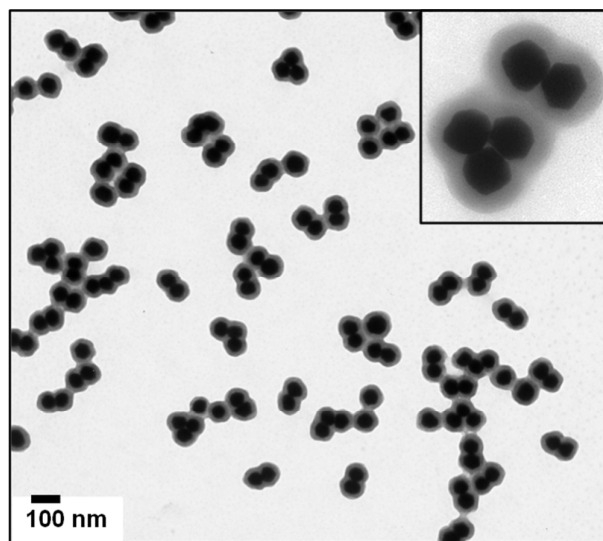


Figure 3: TEM image of a purified colloid containing only small glass-encapsulated clusters of 60 nm AuNPs, in particular dimers and trimers. Inset: high-resolution TEM image.

Single-color immuno-SERS microscopy

SERS-labeled p63 antibodies in conjunction with Raman microscopy were used for localizing the basal cell marker p63 in prostate tissue sections. This protein is abundant in the basal epithelium of the normal prostate, while it is absent in the neoplastic glands.^[21,22] The SERS false color images in Fig. 4 are based on the intensity of the Raman marker band of 4-MBA at about 1590 cm^{-1} (Fig. 2); their size is confined to the corresponding red boxes due to the point mapping approach employed here, in which at each position a Raman spectrum is acquired. The selective abundance of p63 in the basal cells of the epithelium is clearly observable. The hyperplasia of the myoepithelium explains the scattered abundance of the p63 staining. We were not able to observe signals in the secretory epithelium or the

stroma/connective tissue. The staining results in Fig. 4 were obtained with a commercially available antigen retrieval solution; in contrast, we were not able to achieve results of the same or even better quality with home-made demasking buffer.

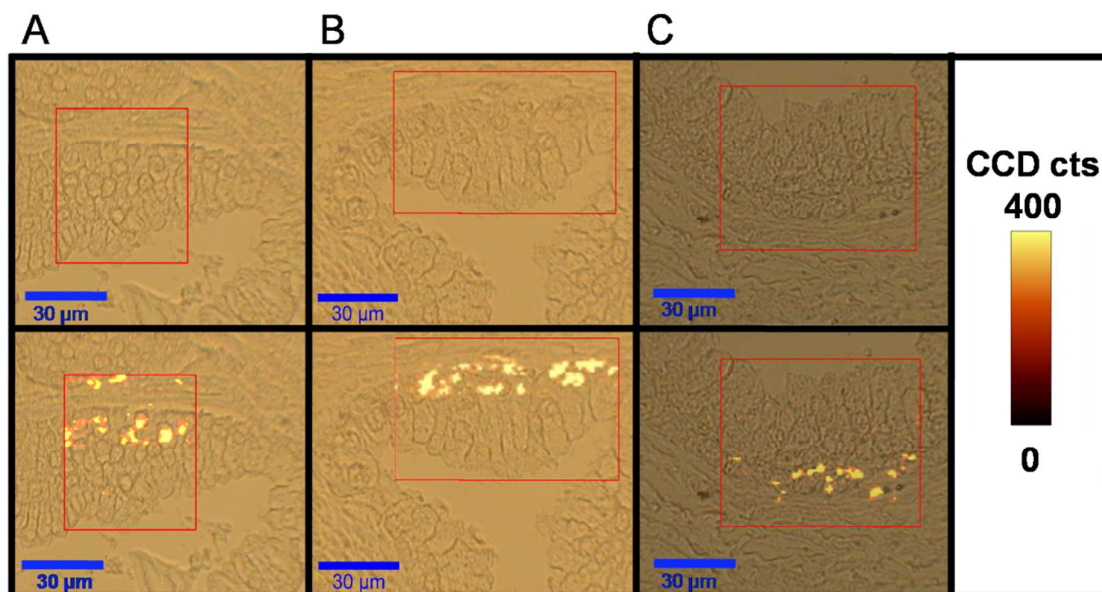


Figure 4: Localization of p63 on non-neoplastic prostate tissue by using SERS-labeled antibodies. White light images (top) and corresponding SERS false-color images (bottom) of three different biopsies (A-C). Acquisition time: 100 msec/pixel.

PSA was chosen as the second target protein because of its high expression levels in prostate tissue and its selective histological abundance in the epithelium of the prostate gland. The localization of PSA in epithelial tissue of the prostate by immuno-SERS microscopy is shown in Fig. 5. The SERS false color images in Fig. 5 are based on the intensity of the Raman marker band of 4-NTB at about 1340 cm^{-1} (Fig. 2).

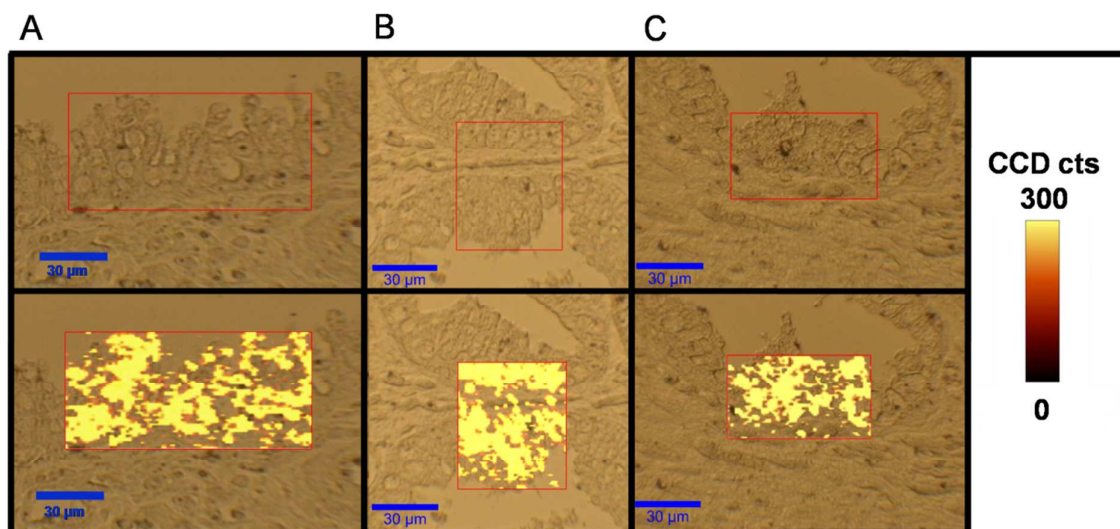


Figure 5: Localization of PSA on tissue by using SERS-labeled PSA antibodies. White light images (top) and corresponding SERS false-color images (bottom) of three different prostate biopsies (A-C). Acquisition time: 100 msec/pixel.

In contrast to the PSA-(+) epithelium, no or only very weak SERS signals are observed in the PSA(-) stroma and lumen. The staining results in Fig. 5 were obtained with a homemade antigen retrieval solution; we were not able to achieve results of the same or even better quality with other buffers.

Two color immuno-SERS microscopy

Two-color immuno-SERS experiments were performed by treating the prostate tissue sections with commercially available antigen retrieval buffer and then incubating them with both SERS-labeled PSA antibodies (Raman reporter: 4-NTB; incubation time: 20 min) and SERS-labeled p63 antibodies (Raman reporter: 4-MBA; incubation time: 12 min) The two-color experiment in Figure 6 confirms the findings from the one-color experiments: p63 is selectively observed in the nuclei of the basal cells, while PSA is abundant in the entire epithelium, but not in the stroma.

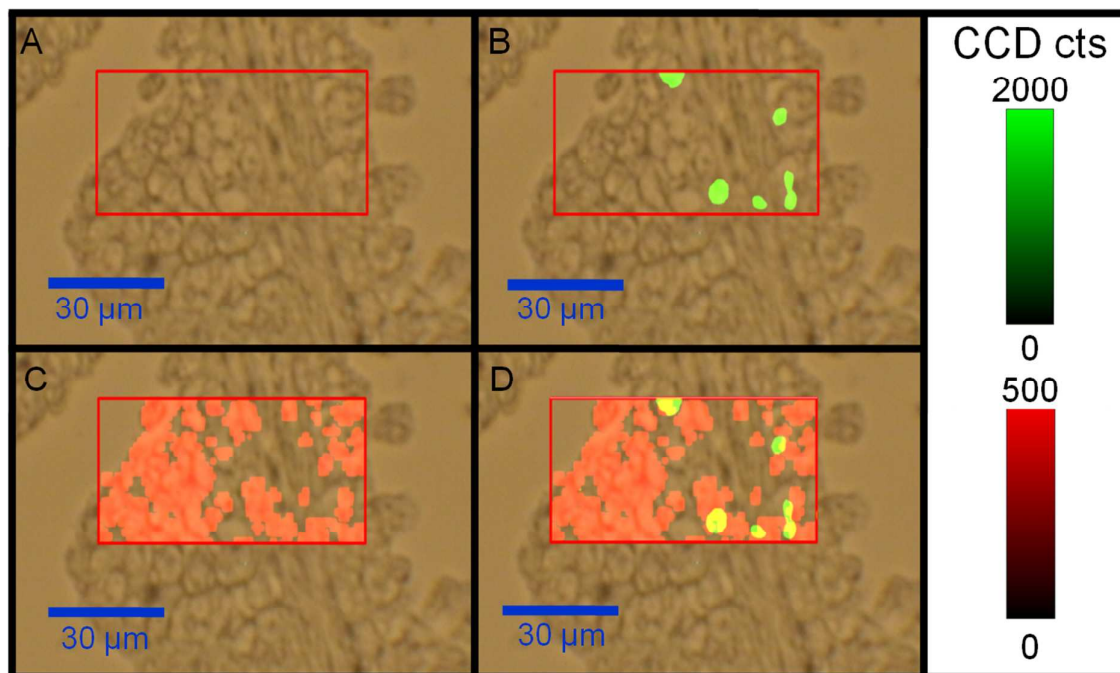


Figure 6: Two-color immuno-SERS microscopy for the co-localization of p63 (green) and PSA (red). White light image of healthy prostate sample (A). Overlay with p63 false-color SERS image; Raman reporter: 4-MBA (B). Overlay with PSA false-color SERS image; Raman reporter: 4-NTB (C). Co-localization by overlay with p63/PSA false-color images (D). A commercially available antigen retrieval solution was employed. Acquisition time: 100 msec/pixel.

Similar to standard IHC, the staining quality in SERS microscopy depends on several factors such as blocking buffers, antigen retrieval, incubation time, and antibody concentration (here: number of nanoparticles). We have examined these parameters in systematic SERS microscopic experiments using gold/silver nanoshells^[1,3,6,24] as SERS labels (Supporting Information, Figs. 1-6) since their chemical preparation and functionalization is much faster compared with the time consuming protocols for the generation (aggregation, silica encapsulation, surface functionalization) and in particular purification (density gradient centrifugation with very small sample amounts) of silica-coated SERS clusters. We have then applied the optimized conditions for gold/silver nanoshells to SERS microscopic experiments employing clusters. The following paragraph describes the role of antigen retrieval methods in detail. For the other parameters (*vide supra*), we refer the reader to the supporting information.

Comparing antigen retrieval methods for co-localization of p63 and PSA

We also tested EDTA-Tris buffer for antigen unmasking. Tissue sections were treated by heating at 95 °C in EDTA-Tris buffer. The intensity of both SERS signals (PSA and p63) was higher compared with Fig. 6 (results not shown). Assuming otherwise comparable conditions, this may indicate a higher number of SERS NPs binding on the tissue. However, a major drawback is that there is considerable nonspecific binding of SERS-labeled PSA antibodies, especially in the PSA(-) stroma. Antigen unmasking with EDTA-Tris therefore seems useful for one-color localization experiments of p63, but not for co-localization of p63 and PSA.

Negative control experiments

Although the p63 results in the one- and two-color immuno-SERS microscopic images clearly indicate the selectivity of the staining approach, we performed negative control experiments employing protein A/G-SERS cluster conjugates (Fig. 7 bottom), i.e., without antibodies, and also SERS clusters conjugated to BSA (Fig. 7 top). Only minor nonspecific binding can be observed in these cases.

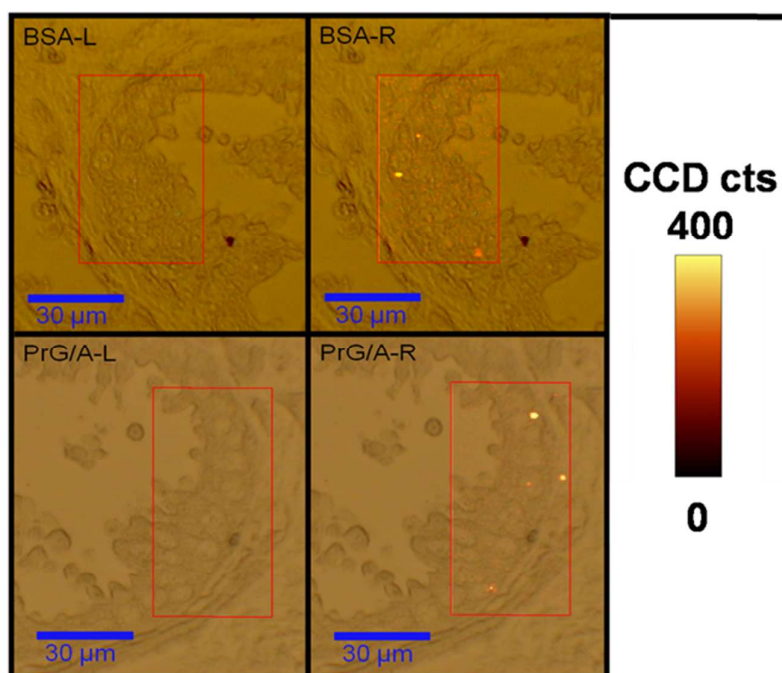


Figure 7: Negative control experiments in immuno-SERS microscopy using SERS NP clusters (Fig. 3) conjugated to either BSA (top) or protein A/G (bottom), respectively. Only minimal nonspecific binding is observed. Acquisition time: 100 msec/pixel.

Positive control experiment

Immunohistochemistry using a primary antibody directed against p63 and horseradish peroxidase (HRP)-labeled protein A/G (instead of a HRP-labeled secondary antibody) was performed as a positive control experiment. The selective staining of the nuclei from the basal cells is clearly visible (Fig. 8). This result demonstrates the selective binding of the p63 primary antibody to the p63 antigen as well as the recognition of the Fc domain of the p63 primary antibody by protein A/G.

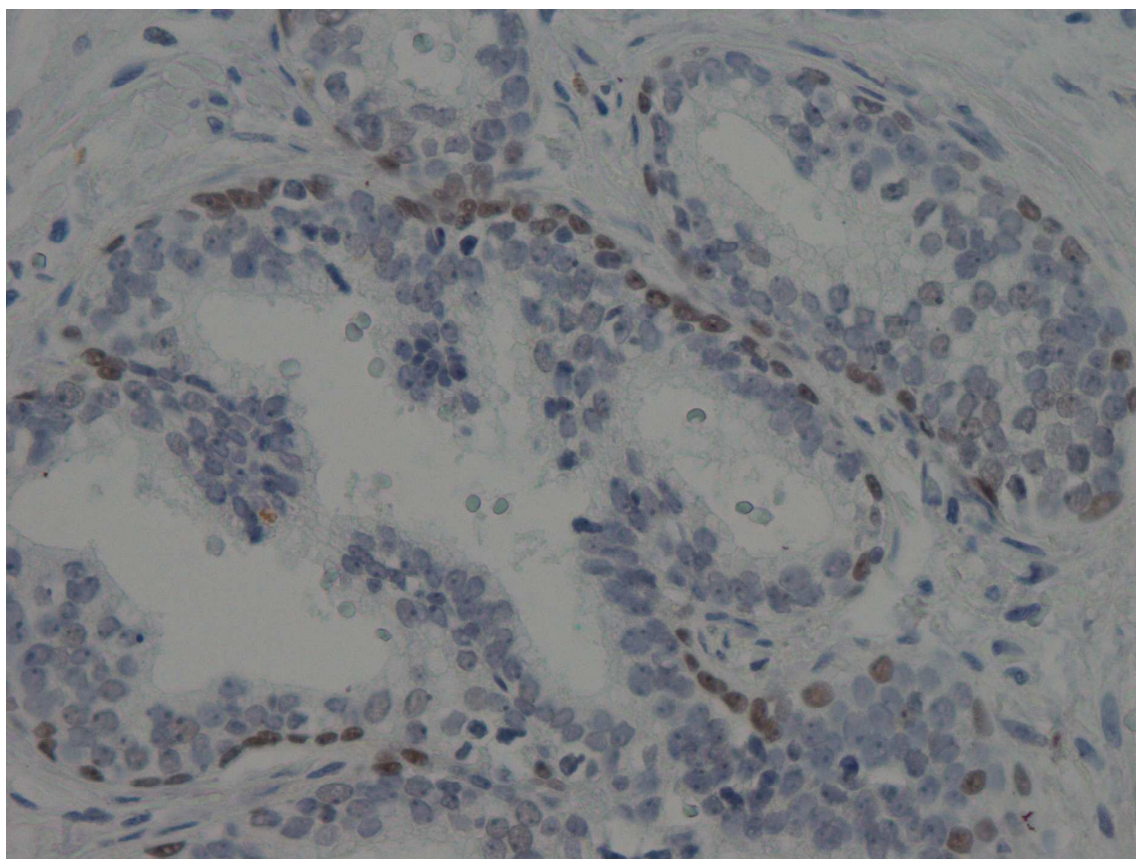


Figure 8: Positive control experiment (immunohistochemistry) using a primary antibody directed against p63 and HRP-labeled protein A/G. The nuclei of the basal cells are selectively stained.

Conclusions and outlook

SERS microscopy is a promising nanodiagnostic approach to immunohistochemistry. The quality of the staining results crucially depends on the physical and chemical properties of the functionalized metal colloids used as SERS labels for bioconjugation to antibodies. In addition, the concentration of SERS nanoparticles, the antigen retrieval method, and the incubation time are further important parameters. In this contribution, we presented small silica-coated clusters of gold nanoparticles as highly SERS-active and bright labels in conjunction with protein A/G coating for noncovalent bioconjugation to antibodies. In contrast to our previous work employing Au/Ag nanoshells^[1,3] and Au nanostars^[4], respectively, the silica-coated clusters of gold nanoparticles are significantly larger and heavier, which probably results in a lower binding affinity. Our proof-of-concept one- and two-color SERS imaging experiments incl. negative controls demonstrate the specific binding of the primary antibody-protein A/G-gold nanocluster conjugates.

In contrast to standard IHC, which employs enzyme-labeled secondary antibodies, SERS microscopy is based on SERS-labeled primary antibodies. This approach saves time and costs during the diagnostic test, and may become crucial for antigen quantification in tissue specimen since an amplification step is obsolete.

Future studies will focus on extending the number of spectrally distinct SERS labels for multiplexed protein localization and also examine to which extent the size/weight of the SERS labels influences the binding efficiency of the corresponding antibody-SERS label-conjugate to its target protein.

Material and Methods:

Ammonia, polyvinylpyrrolidone (PVP), dimethylformamid (DMF), ethanol (EtOH), tetraethoxyorthosilicate (TEOS), 3-amino-n-propyltrimethoxysilane (APTMS), N-hydroxysulfosuccinimide sodium salt (s-NHS), 1-ethyl-3-(3-dimethylaminopropyl) carbodiimide (EDC), isopropanol, succinic anhydride (SAH), Tween 20, Sodium borohydride, 5,5'-Dithiobis(2-nitrobenzoic acid) DTNB and 4-mercaptobenzoic acid (4-MBA) were purchased from Sigma-Aldrich Germany. Polyclonal rabbit antihuman

p63 antigen (α -p63) was obtained from Abcam and the target retrieval solution from DAKO. Monoclonal antihuman PSA (A67-B/E3) was purchased from Zytomed Germany. Protein A/G and HRP-labeled protein A/G were purchased from Thermo Fisher Scientific. Phosphate-buffered saline (PBS: 137mM NaCl, 2.7 mM KCl, 10 mM Na_2HPO_4 , 2 mM KH_2PO_4 , pH 7.4) was prepared in our laboratory. Bovine serum albumin (BSA) and Hepes were purchased from Carl Roth, Germany. In all reaction steps ultrapure water (18.2 M Ω cm) was used.

Preparation of SERS Colloids

Gold nanoparticles: Gold nanoparticles (AuNPs) with an average size of 60 nm (\pm 2 nm) were synthesized by procedures reported previously^[26]. AuNPs were centrifuged at 1500 g for 15 minutes and washed once with a mixture of EtOH and poly-PVP (1000 mg in 40ml). Two different solutions of Raman reporters molecules in ethanol (EtOH) were prepared (3 mg 4-MBA in 2.5 mL EtOH; 3.6 mg DTNB in 2,5 mL EtOH). For cleaving the disulphide bond in DTNB and obtaining the corresponding thiol 4-NTB, sodium borohydride (0.1 mg NaBH_4 in 200 μL EtOH) was added to the DTNB solution. SERS colloids were obtained by incubating the gold colloid with the solution of the Raman reporter molecules. The suspension was incubated over night at room temperature (RT). Uncontrolled aggregation of AuNPs occurred by transferring the Raman-reporter-labeled AuNPs from PVP/EtOH into PBS buffer. The aggregated AuNPs were treated with ultrasound and washed 3 times with water.

Silica encapsulation of aggregated AuNPs: Aggregated AuNPs coated with a SAM of 4-MBA (optical density OD = 1.2) were suspended in 9 mL water. After few seconds, 33 mL isopropanol and 800 μL ammonia were added to the suspension.^[8,23-25] Aggregated AuNPs coated with a SAM of 4-TNB were pretreated 10 minutes with 0,5% APTMS (in ETOH) before the addition of isopropanol and ammonia. Subsequently, 1mL of 1% TEOS solution was slowly added (10 μL TEOS on 990 μL isopropanol) to the SERS colloid. After incubation for 16 h, the encapsulation was completed.

Purification of the silica-encapsulated gold clusters: The silica-encapsulated SERS colloid (crude mixture) was separated by density gradient centrifugation. Five different water/glycerol mixtures (35, 40, 45, 50, and 55% vol-% glycerol) were prepared and stacked on top of each other, starting with the solution containing 35%

vol-% glycerol.^[27] After stacking, the tube was turned horizontally to form a continuous gradient within 5 minutes and pre-centrifuged for 5 minutes at 4890 g. The colloidal sample was added on top of the continuous gradient and centrifuged for 20 minutes at 4890 g in a 14 mL tube. After centrifugation, the silica- encapsulated gold clusters were extracted from the tube with a hypodermic needle by injection through the wall of the plastic. To remove the excess of glycerol, the gold nanoclusters were washed three times (each step: centrifugation followed by redispersion). The final, purified colloid fraction was dispersed in water.

Biofunctionalization of silica-encapsulated AuNP clusters by protein A/G: The purified silica-encapsulated clusters obtained after density gradient centrifugation were then biofunctionalized by protein A/G. In order to hydrolyze the alkoxy silanes on the silica surface of the gold nanoclusters, 120 μ L of ammonia (12,7M) was added and the colloid was treated with ultrasound for 20 minutes. The amino-functionalization was further conducted by adding 30 μ L (0,5%) of APTMS and 30 μ L of ammonia to 1 mL of the colloid, followed by incubation at RT for 30 minutes. Then the clusters were washed with DMF and re-suspended in dry DMF again. Succinic anhydride (0.5 μ g) was added to the cluster suspension. The colloid was treated with ultrasound for 5 minutes and incubated at RT for 20 min. Afterwards, the clusters were centrifuged and washed twice with 50 mM Hepes buffer (pH= 5.8) and suspended in Hepes buffer. Subsequently, 500 μ L of the encapsulated SERS labels (OD 2.5) were activated with 50 μ L of 0.2 % (w/v) s-NHS solution and 50 μ L of 0.3 % (w/v) EDC solution. After incubation for 20 minutes at RT, the clusters were centrifuged and suspended in 300 μ L of Hepes buffer. Five μ g PrA/G were added to silica-encapsulated clusters, followed by incubation at RT for 60 min. After washing 2 times with PBS and 0.2% BSA, the silica-coated gold clusters were re-dispersed in PBS-Tris (20 mM) buffer (pH= 7.2) for IgG conjugation. Two μ g of the corresponding antibody (anti PSA or anti p63) was added to PrA/G-coated AuNP clusters, followed by incubation for 60 min at RT. Afterwards the SERS colloids were washed with PBS and 0.2% BSA (one time) and redispersed in PBS-Tris (20 mM) and 0.2% BSA buffer (pH= 7.2).

Antigen demasking: Paraffin-embedded prostate tissue samples from healthy donors were used for immuno-SERS microscopy. Formalin-fixed tissue (4 μ m thick sections) were treated for 20 minutes with target retrieval solution. Blocking was performed

with 2% BSA in PBS- buffer for 20 min. The tissue was then incubated with 300 μ L p63 antibody-conjugated SERS clusters (OD= 0.2, 200 μ L, dispersed in PBS buffer with 0.2 % BSA) for 12 min. Unbound and non-specifically bound clusters were removed by three time rinsing the tissue section with PBS buffer. The optimal incubation time with PSA antibody-conjugated SERS NPs is around 20 min. For the two-color experiments, we incubated the tissue with SERS NPs in two separate steps. The tissue was incubated with p63 antibody-conjugated SERS NPs first. After washing with PBS buffer once, we incubated the tissue 20 min. with PSA antibody-conjugated SERS NPs. Finally, the tissue was washed three times with PBS buffer to remove non-specifically bound clusters.

Instruments:

Localization of SERS-labeled antibodies was achieved in a mapping experiment with a confocal Raman microscope (WITec Alpha 300R, 30 cm focal length and 600 grooves/mm grating spectrometer) equipped with an EM-CCD. Radiation from the 632.8 nm-line from a HeNe laser was focused onto the sample (5 mW laser power at the sample) by a 40x objective (Olympus) with a numerical aperture of 0.6. Extinction spectra were recorded with a Perkin–Elmer Lambda 35 UV/Vis absorption spectrometer. TEM images were obtained with a Zeiss EM 902 instrument.

References

- [1] Schlücker, S.; Küstner, B.; Punge, A.; Bonfig, R.; Marx, A. and P. Ströbel. Immuno-Raman microspectroscopy: In situ detection of antigens in tissue specimens by surface-enhanced Raman scattering. *J. Raman Spectrosc.* **2006**, *37*, 719–721.
- [2] Lutz, B.; Dentinger, C.; Sun, L.; Nguyen, L.; Zhang, J.; Chmura, AJ.; Allen, A; Chan, S; Knudsen; B. Raman Nanoparticle Probes for Antibody-based Protein Detection in Tissues. *J. Histochem. Cytochem.* **2008**, *56*, 371–379.
- [3] Jehn, C.; Küstner, B.; Adam, B.; Marx, A.; Ströbel, A.; Schmuck, C.; Schlücker, S. Water soluble SERS labels comprising a SAM with dual spacers for controlled bioconjugation. *Phys. Chem. Chem. Phys.* **2009**, *11*, 7499–7504.
- [4] Schütz, M.; Steinigeweg, D.; Salehi, M.; Kömpe, K.; Schlücker, S. Hydrophilically stabilized gold nanostars as SERS labels for tissue imaging of the

tumor suppressor p63 by immuno-SERS microscopy. *Chem. Commun.* **2011**, *47*, 4216-4218.

[5] Kennedy, D.C.; McKay, C.; Tay, L.I.; Rouleau, Y.; Pezacki, P.J.; Carbon-bonded silver nanoparticles: alkyne-functionalized ligands for SERS imaging of mammalian cells. *Chem. Commun.* **2011**, *47*, 3156-3158.

[6] Schlücker, S. SERS Microscopy: Nanoparticle Probes and Biomedical Applications. *ChemPhysChem.* **2009**, *10*, 1344 – 1354.

[7] Wang, Y.; Schlücker S. Rational Design and Synthesis of SERS labels, *Analyst* **2013**, *138*, 2224 – 2238.

[8] Salehi, M.; Steinigeweg, D.; Ströbel, P.; Marx, A.; Packeisen, J.; Schlücker, S. Rapid Immuno-SERS Microscopy for Tissue Imaging with Single Nanoparticle Sensitivity, *J Biophotonics.* **2013**, *6*, 785–792.

[9] Khoury, C.G.; Vo-Dinh, T. Gold Nanostars for Surface-Enhanced Raman Scattering: Synthesis, Characterization and Optimization. *J. Phys. Chem. C.* **2008**, *112*, 18849–18859.

[10] Li, W.; Camargo, P.H.C.; Lu, X.; Xia, Y. Dimers of Silver Nanospheres: Facile Synthesis and Their Use as Hot Spots for Surface-Enhanced Raman Scattering. *Nano Lett.* **2009**, *9*, 1,485-490.

[11] Qian, X.; Li, J.; Nie, S. Stimuli-Responsive SERS Nanoparticles: Conformational Control of Plasmonic Coupling and Surface Raman Enhancement. *J. Am. Chem. Soc.* **2009**, *131*, 7540–7541.

[12] Steinigeweg, D.; Schütz, M.; Schlücker, S. Single gold trimers and 3D superstructures exhibit a polarization-independent SERS response. *Nanoscale* **2013**, *5*, 110-113.

[13] Nakajima, N.; Ikada, Y. Mechanism of amide formation by carbodiimide for bioconjugation in aqueous media. *Bioconjug. Chem.* **1995**, *1*, 123-30.

[14] Yeh, S.W.; Ong, L.J.; Clark, J.H.; Glazer, A.N. Fluorescence properties of allophycocyanin and a crosslinked allophycocyanin trimer. *Cytometry.* **1987**, *1*, 91-5.

[15] Brinkley, M. A brief survey of methods for preparing protein conjugates with dyes, haptens and crosslinking reagents. *Bioconjugate Chem.* **1992**, *1*, 2–13.

[16] Avrameas, S.; Coupling of enzymes to proteins with glutaraldehyde: Use of the conjugates for the detection of antigens and antibodies. *Immunochemistry.* **1969**, *1*, 43–52.

[17] Eliasson, M.; Olsson, A.; Palmcrantz, E.; Wiberg, K.; Inganäs, M.; et al.

Chimeric IgG-binding Receptors Engineered from Staphylococcal Protein A and Streptococcal Protein G. *J. Biol. Chem.* **1988**, *9*, 4323–7.

[18] Eliasson, M.; Andersson, R.; Olsson, A.; Wigzell, H.; Uhlén, M. Differential IgG-binding characteristics of staphylococcal protein A, streptococcal protein G, and a chimeric protein AG. *J. Immunol.* **1989**, *2*, 575–81.

[19] Balk, S.P.; Ko, Y.J.; Bubley, G.J. Biology of prostate-specific antigen. *J. Clin. Oncol.* **2003**, *2*, 383–91.

[20] Abrahamsson, P.A.; Tinzi, M. Do we need PSA and early detection of prostate cancer? *European urology supplements.* **2008**, *5*, 393–395.

[21] Signoretti, S.; Waltregny, D.; Dilks, J.; Isaac, B.; Lin, D.; et al. p63 is a prostate basal cell marker and is required for prostate development. *Am. J. Path.* **2000**, *6*, 1769–1775.

[22] Grisanzio, C.; Signoretti, S.; p63 in prostate biology and pathology. *J. Cell Biochem.* **2008**, *5*, 1354–1368.

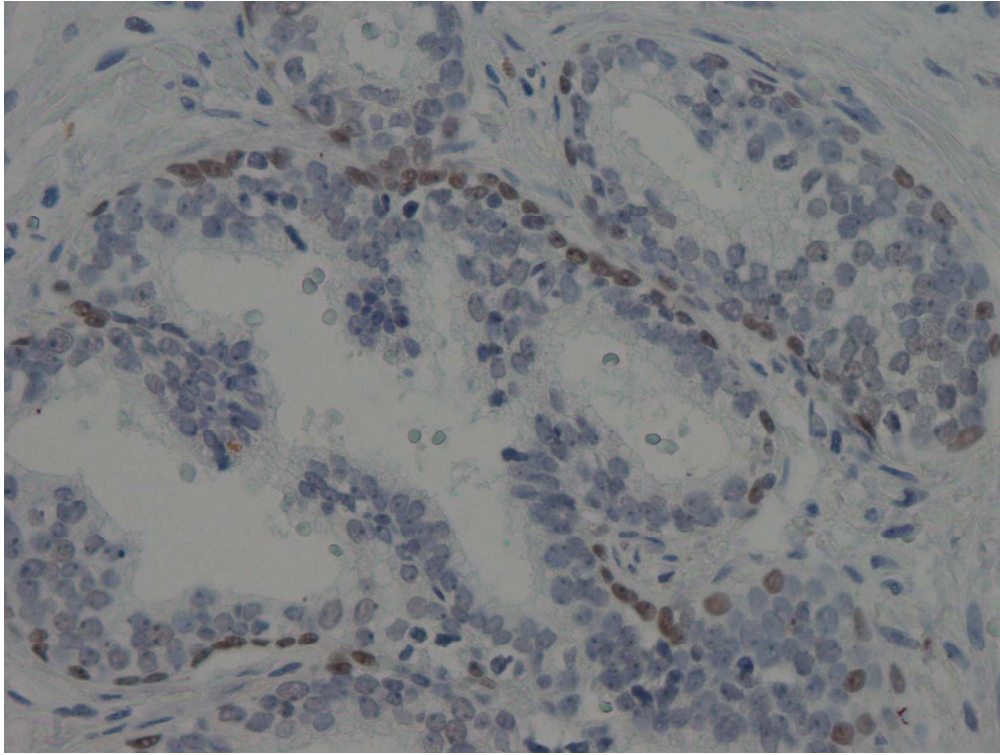
[23] B. Küstner,; M. Gellner,; M. Schütz,; F. Schöppler,; A. Marx,; P. Ströbel,; P. Adam,; C. Schmuck,; S. Schlücker, SERS Labels for Red Laser Excitation: Silica-Encapsulated SAMs on Tunable Gold/Silver Nanoshells, *Angew. Chem. Int. Ed.* **2009**, *48*, 1950–1953.

[24] M. Schütz, B. Küstner, M. Bauer, C. Schmuck, S. Schlücker, Synthesis of Glass-Coated SERS Nanoparticle Probes via SAMs with Terminal SiO₂ Precursors, *Small*, **2010**, *6*, 733-737.

[25] M. Schütz, C. Müller, M. Salehi, C. Lambert, S. Schlücker, Design and synthesis of Raman reporter molecules for tissue imaging by immuno-SERS microscopy, *J. Biophot.* **2011**, *6*, 453–463.

[26] S. D. Perrault,; W. C. W. Chan, Synthesis and Surface Modification of Highly Monodispersed, Spherical Gold Nanoparticles of 50-200 nm, *J. Am. Chem. Soc.* **2009**, *131*, 17042–17043.

[27] D. Steinigeweg,; M. Schütz,; M. Salehi,; S. Schlücker,; Fast and Cost-Effective Purification of Gold Nanoparticles in the 20–250 nm Size Range by Continuous Density Gradient Centrifugation, *Small* **2011**, *10*, 2443-2448.



Two-color Immunohistochemistry based on SERS Microscopy with Primary Antibody Protein A/G-Gold Nanocluster Conjugates is demonstrated